

Coupled Scheme for Linear and Hamilton-Jacobi Equations: Theoretical and Numerical Aspects

Smita Sahu^{1*}

^{1*}School of Mathematics and Physics, University of Portsmouth, Lion Terrace, Portsmouth, PO1 3HF, Hampshire, UK.

Corresponding author(s). E-mail(s): smita.sahu@port.ac.uk;

We present a comprehensive analysis of the coupled scheme introduced in [Springer Proceedings in Mathematics & Statistics, vol 237. Springer, Cham 2018 [23]] for linear and Hamilton-Jacobi equations. This method merges two distinct schemes, each tailored to handle specific solution characteristics. It offers a versatile framework for coupling various schemes, enabling the integration of accurate methods for smooth solutions and the treatment of discontinuities and gradient jumps. In [23], the emphasis was on coupling an anti-dissipative scheme designed for discontinuous solutions with a semi-Lagrangian scheme developed for smooth solutions. In this paper, we rigorously establish the essential properties of the resulting coupled scheme, especially in the linear case. To illustrate the effectiveness of this coupled approach, we present a series of one-dimensional examples.

1 Introduction

In this paper we aim to prove some of the properties of coupled scheme proposed in [23] for first order time dependent Hamilton-Jacobi (HJ) equations. We consider the following one-dimensional Cauchy problem

$$\begin{cases} \partial_t u + H(x, Du) = 0, & (x, t) \in \mathbb{R} \times [0, T], \\ u(x, 0) = u_0(x), & x \in \mathbb{R}, \end{cases} \quad (1)$$

where the Hamiltonian H is convex in the gradient. A classical motivation comes from optimal control theory where $H(x, \nabla u) = \max_{\alpha \in A} \{f(x, \alpha)u_x(t, x)\}$ and α represents the control. It is well known that in this framework the solution u of (1) corresponds to the value function of the corresponding control problem [2, 3]. Typically, solutions

are Lipschitz continuous when the data are Lipschitz continuous. However, in various applications such as control problems with state constraints, games, and image processing, discontinuous solutions are encountered.

In [23], a technique was developed that combines the semi-Lagrangian (*SL*) [13] and ultra-bee (*UB*) [7] scheme to solve both advection problems and HJ equations. Typically, the two initial schemes exhibit distinct characteristics, with one excelling in smooth regions of the solution and the other being more adept at handling discontinuities. The concept behind the coupling scheme is to create a new method that combines the strengths of both schemes without introducing excessive computational costs. This coupling approach is inspired by hybrid schemes used in hyperbolic conservation laws. The choice between methods in the coupled scheme depends on a regularity indicator, incurring a small additional computational cost. It's worth noting that similar couplings are possible, particularly if the schemes use the same nodes. In one dimension, HJ equations are linked to hyperbolic conservation laws, with the viscosity solution of the HJ equation being the primitive of the entropy solution of the corresponding hyperbolic conservation law. Various numerical schemes have been developed for hyperbolic conservation laws (see e.g. [15, 17, 18]), and many of these ideas extend to HJ equations. We also mention that more recently a new class of high-order filtered schemes has been proposed [5] and improved [12], these schemes converge to the viscosity solution and a precise error estimate has been proved. It can be interesting to deal with discontinuous viscosity solutions so these schemes have to be adapted in order to obtain reasonable approximations which do not diffuse too much around the discontinuities of Du and/or u and do not introduce spurious oscillations.

In this paper, we recall the coupled scheme for (1) from [23] based on the coupling between the *UB* scheme (a particular anti-dissipative scheme) and a first order *SL* scheme. Idea is to take the advantage of the properties of the two methods introducing an indicator parameter σ_j^n which will be computed in every cell C_j at every time step in order to detect if there is a singularity or a jump discontinuity there. Then, according to the value of the indicator σ_j^n , we will use the *SL* scheme if the solution is regular enough switching to the *UB* scheme when a discontinuity is detected. It has been discussed in [23] that one of the difficulties in this coupling is that they use different grids and different values: the *SL* scheme computes approximate values at the nodes whereas the *UB* scheme typically works on averaged values which are cell centred, so we have to introduce some projection operators on the grids to switch from one scheme to the other. For schemes working on the same grid and with the same kind of approximate values this projection is not necessary.

Organisation of the paper. In §2, we will recall the *SL* [13] and *UB* [7] schemes and the coupled scheme from [23]. In §3, we will prove some important properties of the coupled *SL + UB* scheme when applied to the linear advection equation. Finally §4, will be devoted to the analysis of some numerical tests in one-dimension for the linear and the nonlinear equation.

2 Background results for the uncoupled schemes.

To make it easier for the reader, we have recall a concise summary of the *SL*schemes by Falcone and Ferretti from [14], the *UB*scheme from [7], and the coupling scheme introduced in [23]. Our notation aligns with that used in [23].

2.1 Semi-Lagrangian Schemes (SL) [13]

In the HJ framework *SL* scheme have been developed initially for the solution of Bellman equations associated with optimal control problems and they can also be interpreted as a discretisation of the dynamic programming principle

In the particular case where the Hamiltonian just depends on the gradient of the solution, i.e. $H(x, Du) = H(Du)$ we have a representation formula for the solution of the Cauchy problem

$$\begin{cases} \partial_t u + H(Du) = 0, & (x, t) \in \mathbb{R} \times [0, T] \\ u(x, 0) = u_0(x), & x \in \mathbb{R}. \end{cases} \quad (2)$$

provided H satisfies (A2) (the so called *Hopf-Lax representation formula*). The *SL* approximation has a strong link with the representation formula, in fact the time discretization can be written as

$$u(x, t + \Delta t) = \min_{a \in \mathbb{R}} \{u(x - a\Delta t, t) + \Delta t H^*(a)\}$$

where

$$H^*(a) = \sup_{p \in \mathbb{R}} \{a \cdot p - H(p)\}$$

is the *Legendre transform* of Hamiltonian H . To get the fully discrete version of the scheme one has to introduce a space discretisation. Let us denote by $I_1[v]$ the P_1 -interpolation (linear interpolation) of a function v in dimension one on the grid $G = \{x_j\}$, i.e. define

$$I_1[v](x) = \frac{x_{j+1} - x}{\Delta x} v_j + \frac{x - x_j}{\Delta x} v_{j+1} \quad \text{for } x \in [x_j, x_{j+1}] \quad (3)$$

The *SL* scheme with P_1 interpolation corresponding to (2) is

$$u_j^{n+1} = \min_{a \in \mathbb{R}} \{I[u^n](x_j - a\Delta t) + \Delta t H^*(a)\} \quad (4)$$

This scheme is monotone, L^∞ -stable and works for the large Courant number. Moreover, convergence and error estimates have been proved (the interested reader can find in [13] a detailed presentation of the theory).

2.2 Ultra-bee (*UB*) scheme for HJ equations

In this section, we recall the *UB* scheme for the HJ equation from [7]. The *UB* scheme is non-monotone and for the transport equation with constant velocity has an interesting

property: it is exact for the class of step functions. We consider the following Cauchy problem

$$\begin{cases} \partial_t u + \max_{\alpha \in \mathcal{A}} \{f(x, \alpha) u_x\} = 0, & (t, x) \in [0, T] \times \mathbb{R} \\ u(x, 0) = u_0(x), & x \in \mathbb{R}, \end{cases} \quad (5)$$

where $f_m := \min_{\alpha \in \mathcal{A}} \{f(x, \alpha)\}$ and $f_M := \max_{\alpha \in \mathcal{A}} \{f(x, \alpha)\}$ equation (5) can be written as

$$\begin{cases} \partial_t u + \max\{f_m(x) u_x, f_M(x) u_x\} = 0, & (t, x) \in [0, T] \times \mathbb{R} \\ u(x, 0) = u_0(x), & x \in \mathbb{R}. \end{cases} \quad (6)$$

Let Δt be a constant time step and $t_n = n\Delta t$ for $n \geq 0$. Given two velocity functions $f_g : \mathbb{R} \rightarrow \mathbb{R}$, where $g = m, M$, we introduce the following notation for the corresponding CFL numbers at a node x_j , $j \in \mathbb{Z}$:

$$\nu_j^m := \frac{\Delta t}{\Delta x} f_m(x_j) \text{ and } \nu_j^M := \frac{\Delta t}{\Delta x} f_M(x_j), \quad (7)$$

Then we can define the infinite vectors, $\nu^m = \{\nu_j^m\}_{j \in \mathbb{Z}}$, $\nu^M = \{\nu_j^M\}_{j \in \mathbb{Z}}$. Now let us define the exact cell average values of the approximate solution at time t_n as

$$\bar{u}_j^n = \frac{1}{\Delta x} \int_{x_{j-1/2}}^{x_{j+1/2}} u(x, t_n) dx, \quad j \in \mathbb{Z}, \quad n \in \mathbb{N}. \quad (8)$$

The *UB* scheme will work on this average values (whereas the *SL* scheme works on point-wise values) typically located at the cell center.. Let $\|f\|_\infty$ denote the L^∞ -norm of a bounded function defined on \mathbb{R} the CFL condition is

$$\max(\|f_m\|_\infty, \|f_M\|_\infty) \frac{\Delta t}{\Delta x} \leq 1. \quad (9)$$

We recall the algorithm for UB scheme 1 from [7, 23]. Note that one can also use the following short representation

$$\bar{u}_j^{n+1} = S_j^{UB}(\bar{u}^n) := \min(\bar{u}_j^{n+1}(\nu^m), \bar{u}_j^{n+1}(\nu^M)), \quad j \in \mathbb{Z} \quad (15)$$

For simplicity we will use the following short notation of *UB* scheme. We recall the simplified flux form of UB scheme which is used in [11] where

$$u_{j+1/2}^n := \bar{u}_j^n + \frac{1 - \nu_j}{\phi_j} (\bar{u}_{j+1}^n - \bar{u}_j^n), \quad (16)$$

where ϕ_j is defined as

$$\phi_j = \begin{cases} \max\left(0, \min\left(\frac{2r_j}{\nu_j}, \frac{2}{1-\nu_j}\right)\right), & \text{if } \bar{u}_{j+1}^n = \bar{u}_j^n \text{ and } \nu_j \neq 1 \\ 0, & \text{otherwise,} \end{cases} \quad (17)$$

Algorithm 1 Algorithm for UB scheme

Initialisation: Compute the initial averages $\{\bar{u}_j^0\}_{j \in \mathbb{Z}}$ as in equation (8) for $n = 0$

Main cycle: For $n \geq 0$, compute $\bar{u}^{n+1} = \{\bar{u}_j^{n+1}\}_{j \in \mathbb{Z}}$ in the following way:

Step 1. For every $j \in \mathbb{Z}$, we define the “fluxes” $u_{j \pm 1/2}^n(\nu_j)$ for $\nu_j \in \{\nu_j^m, \nu_j^M\}$ as follows: for $\nu_j \geq 0$, we define

$$u_{j+1/2}^{n,L}(\nu_j) := \begin{cases} \min(\max(\bar{u}_{j+1}^n, b_j^+(\nu_j)), B_j^+) & \text{if } \nu_j > 0 \\ \bar{u}_{j+1}^n & \text{if } \nu_j = 0 \text{ and } \bar{u}_j^n \neq \bar{u}_{j-1}^n \\ \bar{u}_j^n & \text{if } \nu_j = 0 \text{ and } \bar{u}_j^n = \bar{u}_{j-1}^n \end{cases} \quad (10)$$

where

$$\begin{cases} b_j^+(\nu_j) := \max(\bar{u}_j^n, \bar{u}_{j-1}^n) + \frac{1}{\nu_j} (\bar{u}_j^n - \max(\bar{u}_j^n, \bar{u}_{j-1}^n)), \\ B_j^+(\nu_j) := \min(\bar{u}_j^n, \bar{u}_{j-1}^n) + \frac{1}{\nu_j} (\bar{u}_j^n - \min(\bar{u}_j^n, \bar{u}_{j-1}^n)), \end{cases} \quad (11)$$

for $\nu_j < 0$, we define

$$u_{j-1/2}^{n,R}(\nu_j) := \begin{cases} \min(\max(\bar{u}_{j-1}^n, b_j^-(\nu_j)), B_j^-) & \text{if } \nu_j < 0 \\ \bar{u}_{j-1}^n & \text{if } \nu_j = 0 \text{ and } \bar{u}_j^n \neq \bar{u}_{j+1}^n \\ \bar{u}_j^n & \text{if } \nu_j = 0 \text{ and } \bar{u}_j^n = \bar{u}_{j+1}^n \end{cases} \quad (12)$$

where

$$\begin{cases} b_j^-(\nu_j) := \max(\bar{u}_j^n, \bar{u}_{j+1}^n) + \frac{1}{\nu_j} (\bar{u}_j^n - \max(\bar{u}_j^n, \bar{u}_{j+1}^n)), \\ B_j^-(\nu_j) := \min(\bar{u}_j^n, \bar{u}_{j+1}^n) + \frac{1}{\nu_j} (\bar{u}_j^n - \min(\bar{u}_j^n, \bar{u}_{j+1}^n)), \end{cases} \quad (13)$$

Step 2. For $\nu_j \in \{\nu_j^m, \nu_j^M\}$, we define the flux form of the *UB* scheme

$$\bar{u}_j^{n+1} = \bar{u}_j^n - \nu_j \left(u_{j+1/2}^{n,L}(\nu) - u_{j-1/2}^{n,R}(\nu) \right) \quad (14)$$

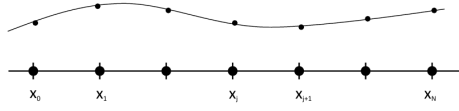
Step 3. Finally, we set $\bar{u}_j^{n+1} := \min(\bar{u}_j^{n+1}(\nu_j^m), \bar{u}_j^{n+1}(\nu_j^M))$, $j \in \mathbb{Z}$.

where $r_j = \frac{\bar{u}_j^n - \bar{u}_{j-1}^n}{\bar{u}_{j+1}^n - \bar{u}_j^n}$. Replacing $j = j - 1$ we can compute $u_{j-1/2}^n$.

Finally, as we said, the *UB* scheme has been proved to transport exactly step functions when the velocity is constant. We will see in §3 that it can be written in an incremental form and this will be useful in some proofs.

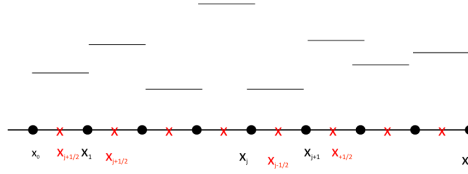
2.3 Coupled scheme [23]

As previously mentioned, *UB* scheme build upon prior conservation law results and typically involve a discontinuous reconstruction at each step. While this choice proves effective in non-regular solution regions, it falls short in regular solution areas. Therefore, a promising approach is to blend the strengths of two schemes: one (*SL*) well-suited for regular (at least Lipschitz continuous) solutions and an *UB* scheme that excels in preserving solution profiles at jumps. By combining these two schemes,



Grid for semi-Lagrangian Scheme

(a) $G^{SL} := \{x_j : x_j = j\Delta x, j = \mathbb{Z}\}$



Grid for Antidiffusive Scheme

(b) $G^{UB} := \{\bar{x}_j : \bar{x}_j = x_j + \frac{\Delta x}{2}, j \in \mathbb{Z}\}$.

Fig. 1: The two grids for SL and UB schemes.

we anticipate obtaining several advantages. To achieve this, we need the ability to identify both regular and singular regions. The SL scheme employs a local interpolation operator to recover the numerical solution's value at the points where characteristics intersect the grid, rather than using cell averages, as is the case with UB schemes. For coupling we need two different grids G^{SL} and G^{UB} give in Fig. 1. \bullet -nodes the nodes of G^{SL} and \times -nodes the nodes of G^{UB} . In the sequel u_j^n denotes an approximation of $u(x_j, t_n)$, and \bar{u}_j^n denotes an approximation of $\bar{u}(\bar{x}_j, t_n)$, where $t_n = n\Delta t$, $\Delta t > 0$. Moreover, we will drop the time index n and denote for simplicity $u_j = u_j^n$ whenever the time dependence is not necessary. At every step, we divide our domain into two regions, one where our approximate solution is “regular” and the other where we detect discontinuities. In order to make the readability and simplicity we recall all the definitions from [23]. Left and right derivatives for every node $x_j \in G^{SL}$

$$D^-u_j := \frac{u_j - u_{j-1}}{\Delta x} \quad \text{and} \quad D^+u_j := \frac{u_{j+1} - u_j}{\Delta x} \quad (18)$$

Definition 1 (Regular cell). *Let δ be a positive threshold parameter. A cell $C_j = [x_j, x_{j+1})$ is said to be a regular cell if we have $|Du_j| < \delta$, $Du_j Du_{j-1} > 0$ and $Du_j Du_{j+1} > 0$.*

This means that a derivative below a given threshold as well as a constant sign in the derivatives just before and after the node x_j is considered to be a regularity indicator. For the choice of the threshold δ we can use a previous knowledge of the bounds for the exact solution. For example, in the case of transport equation with the

constant velocity, we know the solution which is $u(x, t) = u_o(x - ct)$, so we can set our threshold with the help of the initial condition $\delta = \|Du_o^0\|_\infty - \epsilon$, $\epsilon > 0$.

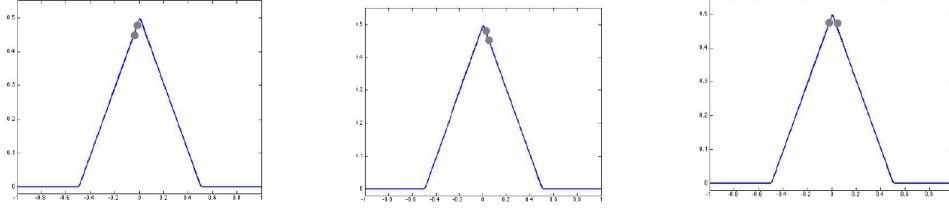


Fig. 2: A sketch of three possible situations around a jump of the derivative.

Definition 2 (Singular cell.). *A cell C_j is said to be a singular cell if it is not a regular cell. We denote the set of singular cells by C_s .*

Definition 3 (Singular and regular region). *The singular region Ω_{sin} is defined by the union of all the singular cells. The set $\Omega_{reg} = \mathbb{R} \setminus \Omega_{sin}$ is called the regular region.*

We need to distinguish between the nodes $x_j \in G^{SL}$ belonging to one of the above regions in order to apply the more adapt scheme there. To this end we define the *regularity indicator*, which will govern the switching between the two schemes: $\sigma_j \equiv 0$ for $x_j \in \Omega_{sin}$ and $\sigma_j \equiv 1$ for $x_j \in \Omega_{reg}$.

Definition 4 (Local Projection Operator for SL). *We define the local projection operator $P^{SL} : \mathbb{R}^2 \rightarrow \mathbb{R}$ by a map which defines the new value u_j at x_j starting from the values $(\bar{u}_{j-1/2}, \bar{u}_{j+1/2})$,*

$$P^{SL}(\bar{u}_{j-1/2}, \bar{u}_{j+1/2}) := \frac{\bar{u}_{j-1/2} + \bar{u}_{j+1/2}}{2} = u_j \quad (19)$$

The P^{SL} operator constructs the point value at x_j as the average of the averaged values at \bar{x}_{j-1} and \bar{x}_j .

Definition 5 (Local Projection Operator for UB). *We define the local projection operator $P^{UB} : \mathbb{R}^2 \rightarrow \mathbb{R}$ by a map which defines the new value \bar{u}_j at $x_{j+1/2}$ starting from the values (u_j, u_{j+1}) ,*

$$P^{UB}(u_j, u_{j+1}) := \frac{u_j + u_{j+1}}{2} = \bar{u}_{j+1/2}. \quad (20)$$

The P^{UB} operator constructs the averaged value at \bar{x}_j as the average of the point values at x_j and x_{j+1} .

The projection operators will be used locally whenever in a cell we switch from one scheme to the other and we need new values which were not available before. The P^{SL} operator will also be used at Step 5 to allow the up-date of the regularity indicator which is computed on the \bullet -nodes. In the sequel we will consider an initial condition w^0 with compact support Q and define the subset $J := [j_{min}, j_{max}] \subset \mathbb{Z}$ containing the

node indices of an interval containing Q . Now we will give the algorithm for coupled scheme 2 from [23]

Algorithm 2 Algorithm for the Coupled ($SL+UB$) scheme

Initialisation: We compute the initial data $w_j^0 = u_j^0$ on every x_j , $j \in J$.

We compute $D^-w_{j-1}^0$, $D^-w_j^0$ and $D^-w_{j+1}^0$ and check the condition

$$|D^-w_j^0| < \delta \text{ and } D^-w_{j-1}^0 D^-w_j^0 > 0, \quad D^-w_j^0 D^-w_{j+1}^0 > 0. \quad (21)$$

if condition (21) is true then we set $\sigma_j^0 = 1$ else $\sigma_j^0 = 0$.

Main cycle on $j \in J$, For $n > 0$.

Step 1. We compute $D^-w_{j-1}^n$, $D^-w_j^n$ and $D^-w_{j+1}^n$ and check the condition

$$|D^-w_j^n| < \delta \text{ and } D^-w_{j-1}^n D^-w_j^n > 0, \quad D^-w_j^n D^-w_{j+1}^n > 0. \quad (22)$$

If condition (22) is true then go to Step 2 else we go to Step 3.

Step 2. We apply the SL scheme at x_j and set $\sigma_j^n = 1$ at the node x_j .

If $\sigma_j^n = \sigma_j^{n-1}$ we directly compute the new value according to the SL scheme

$$w_j^{n+1} = \sigma_j^n S_j^{SL}[w^n] + (1 - \sigma_j^n) S_j^{UB}[w^n] = S_j^{SL}[w^n]. \quad (23)$$

If $\sigma_j^n \neq \sigma_j^{n-1}$, we have to switch from the AD -scheme to the SL scheme and we need the projection P^{SL} . Then, we set for $k = j, j + 1$

$$w_k^n = P^{SL}(\bar{u}_{k-1/2}^n, \bar{u}_{k+1/2}^n) := \frac{\bar{u}_{k-1/2}^n + \bar{u}_{k+1/2}^n}{2} = u_k^n$$

and we compute

$$w_j^{n+1} = \sigma_j^n S_j^{SL}[w^n] + (1 - \sigma_j^n) S_j^{UB}[w^n] = S_j^{SL}[w^n], \quad (24)$$

If $\sigma_j^n \neq \sigma_j^{n-1}$, we have to switch from the AD -scheme to the SL scheme and we need the projection P^{SL} . Then, we set for $k = j, j + 1$

$$w_k^n = P^{SL}(\bar{u}_{k-1/2}^n, \bar{u}_{k+1/2}^n) := \frac{\bar{u}_{k-1/2}^n + \bar{u}_{k+1/2}^n}{2} = u_k^n$$

and we compute

$$w_j^{n+1} = \sigma_j^n S_j^{SL}[w^n] + (1 - \sigma_j^n) S_j^{UB}[w^n] = S_j^{SL}[w^n], \quad (25)$$

Step 4. The condition (22) is not satisfied, then we set $\sigma_j^n = 0$.

If $\sigma_j^n = \sigma_j^{n-1}$ we directly compute the new value according to the *AD*-scheme

$$\bar{w}_j^{n+1} = \sigma_j^n S_j^{SL}[w^n] + (1 - \sigma_j^n) S_j^{UB}[w^n] = S_j^{UB}[w^n]. \quad (26)$$

If $\sigma_j^n \neq \sigma_j^{n-1}$, we have to switch from the *SL*-scheme to the *AD*-scheme and we need the projection P^{UB} . Then, we set for $k = j - 1, j, j + 1$

$$\bar{w}_k^n = P^{UB}(u_k^n, u_{k+1}^n) := \frac{u_k^n + u_{k+1}^n}{2} = \bar{u}_{k+1/2}^n$$

and we compute

$$\bar{w}_j^{n+1} = \sigma_j^n S_j^{SL}[w^n] + (1 - \sigma_j^n) S_j^{UB}[\bar{w}^n] = S_j^{UB}[\bar{w}^n], \quad (27)$$

End of the j cycle.

Step 5 (Filling the holes procedure)

At the \bullet -nodes where $\sigma_j^n = 0$ we need to project by P^{SL} defined in (19) using the intermediate values at \bar{w}_{j-1}^{n+1} and \bar{w}_j^{n+1} , i.e.

$$w_j^{n+1} = P^{SL}(\bar{w}_{j-1}^{n+1}, \bar{w}_j^{n+1}), \text{ for } \sigma_j = 0.$$

(the values w_j^{n+1} for the \bullet -nodes where $\sigma_j = 1$ are already available by Step 4). This will finally produce the new approximate solution w_j^{n+1} .

Step 6 Set $n = n + 1$, $j = j_{min}$ and go back to the Main cycle. \square

Note that at the \bullet -nodes where $\sigma_j^n = 1$ we always have a value which is computed by the *SL* scheme and that the switching indicator is chosen on the basis of the values at the \bullet -nodes.

3 Some properties of the coupled *SL+UB* scheme

This section is devoted to the analysis of some interesting properties for the coupled scheme. We will study these properties for the advection problem, the extension to the non linear problem is rather difficult and is still under study. However, at the end of the paper we will present also a test for an HJ equation which shows that the coupling procedure is also effective for nonlinear problems and deserves further analysis. Let us start introducing some classical definitions.

Definition 6. The Discrete Total Variation of a vector $u = \{u_j\}_{j \in \mathbb{Z}}$ is given by

$$TV(u) := \sum_{j \in \mathbb{Z}} |u_j^n - u_{j+1}^n|. \quad (28)$$

This definition is the discrete analogue of the continuous total variation for a continuous function.

Definition 7. We say that a scheme is Total Variation Diminishing (TVD) if for all $n \geq 0$,

$$TV(u^{n+1}) \leq TV(u^n). \quad (29)$$

where u^n is the approximate solution at time t_n .

Definition 8. We say that a scheme is Total Variation Bounded (TVB) if for any initial condition such that $TV(u^0) < \infty$ and time T there exists a positive constant C , and a value Δt_0 such that

$$TV(u^n) \leq C \quad (30)$$

for all $n\Delta t \leq T$ whenever $\Delta t < \Delta t_0$ (again u^n denotes the approximate solution at time t_n).

This definitions dates back to the first papers on high-order approximation schemes for scalar conservation laws (see [17, 18]). The fact that the total variation is decreasing in time is a typical feature of entropy solution to scalar conservation laws. Moreover, the control of the total variation gives a control on the oscillations of the scheme. For a detailed analysis of the role of the above property in the analysis of high-order approximation schemes we refer to the monographs [20] and [16]. Following Harten [18] say that a *scheme is in incremental form* if it can be written as

$$u_j^{n+1} = u_j^n - C_{j-\frac{1}{2}}(u_j^n - u_{j-1}^n) + D_{j+\frac{1}{2}}(u_{j+1}^n - u_j^n), \quad (31)$$

where $C_{j-\frac{1}{2}}, D_{j+\frac{1}{2}} \in \mathbb{R}$. We recall [17] that a scheme in incremental form is TVD if and only if the following sufficient conditions are satisfied for all j :

$$0 \leq C_{j-\frac{1}{2}}, D_{j+\frac{1}{2}} \text{ and } C_{j-\frac{1}{2}} + D_{j+\frac{1}{2}} \leq 1. \quad (32)$$

For the *UB* scheme it is relevant to recall the following definitions.

Definition 9. The *UB* scheme is L^∞ -stable if the following conditions hold:

$$\text{for } \nu_j \geq 0, \min(u_j^n, u_{j-1}^n) \leq u_j^{n+1} \leq \max(u_j^n, u_{j-1}^n), \quad (33)$$

$$\text{for } \nu_j < 0, \min(u_j^n, u_{j+1}^n) \leq u_j^{n+1} \leq \max(u_j^n, u_{j+1}^n). \quad (34)$$

It is clear that above definition of L^∞ -stability implies the standard definition of L^∞ -stability which requires

$$\|u^n\|_{L^\infty} \leq C \|u^0\|_{L^\infty}, \forall n \in \mathbb{N} \quad (35)$$

Infact, by definiton 9 one gets

$$-\|u^n\|_\infty \leq \min(u_{j-1}^n, u_j^n, u_{j+1}^n) \leq u_j^{n+1} \leq \max(u_{j-1}^n, u_j^n, u_{j+1}^n) \leq \|u^n\|_\infty \quad (36)$$

which easily implies (35).

Definition 10. We say that *UB* shceme is consistent if all the fluxes $u_{j+\frac{1}{2}}^{n,L}$ and $u_{j+\frac{1}{2}}^{n,R}$ satisfy:

$$\text{for } \nu_j \geq 0, \min(\bar{u}_j^n, \bar{u}_{j-1}^n) \leq u_{j+\frac{1}{2}}^{n,L} \leq \max(\bar{u}_j^n, \bar{u}_{j-1}^n), \quad (37)$$

$$\text{for } \nu_j < 0, \min(\bar{u}_j^n, \bar{u}_{j+1}^n) \leq u_{j+\frac{1}{2}}^{n,R} \leq \max(\bar{u}_j^n, \bar{u}_{j+1}^n). \quad (38)$$

As we said, if $|\nu_j| \leq 1$ for every j , the UB scheme is consistent, L^∞ stable and TVD. These properties will now be extended to the coupled scheme using the definition of our projection operators on the two grids G^{SL} and G^{UB} .

Properties of the Coupled Scheme for the advection equation

Let us consider the following model problem

$$\begin{cases} u_t + cu_x = 0, & x \in \mathbb{R}, t \in [0, T] \\ u(x, t) = u_0(x) \end{cases} \quad (39)$$

where c is a constant velocity. In the following, we will continue to use the notations u_j^n , \bar{u}_j^n and w_j^n respectively for the values computed by the SL , UB and coupled scheme at time n and at the node j of their respective grids (shifted by $\Delta x/2$). We consider the particular coupled scheme obtained by a the SL scheme and the UB scheme:

$$w_j^{n+1} = \sigma_j^n S_j^{SL}[w^n] + (1 - \sigma_j^n) S_j^{UB}[w^n], \quad (40)$$

with the two projections (19) or (20) (as explained in the coupled scheme algorithm we use projection only when it is needed by σ_j^n). When we are in the regular region the above coupled scheme coincides with the SL scheme. For $c > 0$, let $\nu := c \frac{\Delta t}{\Delta x} < 1$, we have $x_j - c\Delta t \in (x_{j-1}, x_j]$ obtaining the following SL scheme

$$w_j^{n+1} = u_j^{n+1} = S_j^{SL}(u^n) := \nu u_{j-1}^n + (1 - \nu) u_j^n \quad (41)$$

Although Δt can in general be rather big as SL schemes typically work for large Courant numbers here we will set $\nu = 1$ because the coupling is made with the UB scheme which needs that condition for stability. This limitation will be compensated by the higher accuracy at the jumps given by the UB scheme. Note that the following properties of the projection operators play an important role:

$$\min(u_j^n, u_{j+1}^n) \leq \bar{u}_j^n = P^{UB}(u_j^n, u_{j+1}^n) = \frac{u_j^n + u_{j+1}^n}{2} \leq \max(u_j^n, u_{j+1}^n) \quad (42)$$

$$\min(\bar{u}_j^n, \bar{u}_{j+1}^n) \leq u_j^n = P^{SL}(\bar{u}_j^n, \bar{u}_{j+1}^n) = \frac{\bar{u}_j^n + \bar{u}_{j+1}^n}{2} \leq \max(\bar{u}_j^n, \bar{u}_{j+1}^n) \quad (43)$$

In order to clarify which values are really involved in the computation we will keep the notations with u and \bar{u} instead of w . However, these values are computed according to the coupled algorithm already described in §3.

Proposition 1. *Let us consider the advection problem (39) and let $|\nu| \leq 1$. The coupled scheme $SL+UB$ is L^∞ -stable.*

Proof. Note that for a constant velocity c , choosing $\lambda = \Delta t/\Delta x$ small enough the parameter ν will be always lower than 1. This means that only the first neighbouring cells will appear in the stencil for the SL and for the UB scheme. We will consider four cases at a generic node x_j : two are related to the situation where the parameter σ_j^n remains constant passing from step t_{n-1} to t_n whereas the remaining two cases

refer to the switching case.

Case 1: $\sigma_j^n = \sigma_j^{n-1} = 1$, i.e. no switch is needed. We continue to apply at the node x_j the *SL* scheme with local piecewise linear reconstruction on the neighbouring cells $[x_{j-1}, x_j]$ and $[x_j, x_{j+1}]$ so

$$\min(u_{j-1}^n, u_j^n, u_{j+1}^n) \leq u_j^{n+1} \leq \max(u_{j-1}^n, u_j^n, u_{j+1}^n).$$

and this implies the same for w .

Case 2: $\sigma_j^n = \sigma_j^{n-1} = 0$, i.e. no switch is needed. We continue to apply the *UB* scheme and the property at the node j comes from the fact that the *UB* scheme satisfies the stability property (9).

Case 3: $\sigma_j^n = 1$ and $\sigma_j^{n-1} = 0$. We switch from the *UB* scheme to the *SL* scheme so we need to use local projection operator (19). More precisely, we assign (if necessary) to the \bullet -nodes x_{j-1} , x_j and x_{j+1} the values obtained by averaging the values computed by the *UB* scheme at the corresponding \times -nodes and we apply the *SL* scheme to compute u_j^{n+1} . This will produce a new value satisfying

$$\min(\bar{u}_j^n, \bar{u}_{j+1}^n) \leq u_j^{n+1} \leq \max(\bar{u}_j^n, \bar{u}_{j+1}^n)$$

which by construction implies

$$\min(u_{j-1}^n, u_j^n, u_{j+1}^n) \leq u_j^{n+1} \leq \max(u_{j-1}^n, u_j^n, u_{j+1}^n).$$

Case 4: $\sigma_j^n = 0$ and $\sigma_j^{n-1} = 1$. We switch from the *SL* scheme to the *UB* scheme so we need to use the local projection operator (20). More precisely, the values u_j^n has been computed by *SL* scheme because $\sigma_j^{n-1}=1$ and we assume that also the neighbouring values u_{j-1}^n and u_{j+1}^n are available (if not they can be obtained averaging by the projection operator P^{UB} (20)).

This gives

$$P^{UB}(w_{j-1}^n, w_j^n) = P^{UB}(u_j^n, u_{j+1}^n) = \frac{u_j^n + u_{j+1}^n}{2} = \bar{u}_j^n, \quad (44)$$

and since $\sigma_j^n = 0$ the coupled scheme will compute the value

$$w_j^{n+1} = S_j^{UB}[w^n] \quad (45)$$

Then the L^∞ bound is satisfied by (42) and the stability property of the *UB* scheme. \square

Proposition 2. *We consider the advection problem (39) and let $|\nu| \leq 1$. The coupled scheme *SL+UB* is TVB.*

Proof. To prove the TVB property we still have to examine four cases as in the previous proposition. We will give the proof for $\nu \geq 0$, when ν is negative the proof

can be easily adapted. As we will see, in some cases when we do not switch we will have a stronger property, i.e. the scheme will be TVD. When we have a switch we just have the TVB property.

Case 1: For $\sigma_j^n = \sigma_j^{n-1} = 1$ for every j , so no switch is needed and we will always apply SL at all the nodes. Let us prove that the scheme is TVD. We have

$$u_j^{n+1} = w_j^{n+1} = S_j^{SL}[w^n] \quad (46)$$

which means

$$u_j^{n+1} = \nu u_{j-1}^n + (1 - \nu)u_j^n \quad (47)$$

where $\nu \in (0, 1]$. So for the difference we get

$$\begin{aligned} |u_{j+1}^{n+1} - u_j^{n+1}| &= |\nu u_j^n + (1 - \nu)u_{j+1}^n - (\nu u_{j-1}^n + (1 - \nu)u_j^n)| \leq \\ &\leq |\nu(u_j^n - u_{j-1}^n) + (1 - \nu)(u_{j+1}^n - u_j^n)| \end{aligned} \quad (48)$$

Summing on j we obtain

$$\sum_{j \in \mathbb{Z}} |u_{j+1}^{n+1} - u_j^{n+1}| \leq \sum_{j \in \mathbb{Z}} |\nu(u_j^n - u_{j-1}^n) + (1 - \nu)(u_{j+1}^n - u_j^n)| \quad (49)$$

so

$$TV(u^{n+1}) \leq \nu TV(u^n) + (1 - \nu)TV(u^n) \quad (50)$$

for $\nu \in [0, 1]$, which implies for the approximate solution of the coupled scheme

$$TV(w^{n+1}) = TV(u^{n+1}) \leq TV(u^n) = TV(w^n). \quad (51)$$

Case 2: For $\sigma_j^n = \sigma_j^{n-1} = 0$ for every j , so no switch is needed and we will always apply UB at all the nodes. For $\nu \geq 0$ we have

$$w_j^{n+1/2} = S_j^{UB}[w^n] \quad (52)$$

so we can also write for every $j \in \mathbb{Z}$

$$w_j^{n+1} = \bar{u}_j^{n+1} = \bar{u}_j^n - C_{j-1/2}(\bar{u}_j^n - \bar{u}_{j-1}^n)$$

with $C_{j-1/2} \in [0, 1]$, i.e. (31) with $D_{j+1/2} = 0$. Hence we have the incremental form (31) with $C_{j+1/2} + D_{j+1/2} \leq 1$. Thus the scheme is TVD. For $\nu < 0$ we will have the a similar expression where the coefficient $C_{j+1/2}$ vanishes and $D_{j+1/2} > 0$, so again we will have the TVD property.

Case 3: $\sigma_j^n = 1$ and $\sigma_j^{n-1} = 0$. In addition, we assume that $\sigma_{j-1}^n = 1$. The scheme switches at x_j from the UB to SL . For $\nu \geq 0$, let us examine the total variation in the interval $D = [x_{j-1}, x_{j+1}]$, i.e. in the union of cells whose nodes are used in the switch.

We define $J := \{j-1, j\}$ and we denote by $Var_A(w)$ the variation of a vector w over A , i.e.

$$Var_J(w) := \sum_{k=j-1}^j |w_k - w_{k+1}| \quad (53)$$

Recalling the definition of P^{SL} we have

$$Var_J(w^{n+1}) = \sum_{k=j-1}^j |w_k^{n+1} - w_{k+1}^{n+1}| \quad (54)$$

$$\begin{aligned} &= |w_{j-1}^{n+1} - w_j^{n+1}| + |w_j^{n+1} - w_{j+1}^{n+1}| \quad (55) \\ &= \left| u_{j-1}^{n+1} - \frac{\bar{u}_{j-1}^{n+1} + \bar{u}_j^{n+1}}{2} \right| + \left| \frac{\bar{u}_{j-1}^{n+1} + \bar{u}_j^{n+1}}{2} - u_{j+1}^{n+1} \right| \end{aligned}$$

If there is a switch from SL to UB scheme then by equation (21) and (22), we have

$$|D^- w_j| > \delta.$$

If we are in regular region that means $\sigma_j^n = 1$ then we have

$$\left| \frac{w_j^n - w_{j-1}^n}{\Delta x} \right| < \delta \Rightarrow |w_j^n - w_{j-1}^n| < \delta \Delta x$$

Now we apply the SL scheme to these nodes and we assume $\nu \geq 0$ (the opposite sign can be treated in a similar way). For every $k \in A$ we have

$$w_k^{n+1} = S_k^{SL}[w^n] = \nu w_{k-1}^n + (1 - \nu)w_k^n \quad (56)$$

Now we want to obtain a bound for $Var_J(w^{n+1})$. By applying (56) and simply reordering the terms as we have done in the above proof of Case 1, we have

$$Var_A(w^{n+1}) = \sum_{k=j-1}^j |\nu(w_{k-1}^n - w_k^n) + (1 - \nu)(w_k^n - w_{k+1}^n)| \quad (57)$$

which implies, since ν and $(1 - \nu) \in [0, 1]$,

$$\begin{aligned} Var_A(w^{n+1}) &\leq |w_{j-2}^n - w_{j-1}^n| + |w_{j-1}^n - w_j^n| + |w_j^n - w_{j+1}^n| \quad (58) \\ &\leq |w_{j-2}^n - w_{j-1}^n| + Var_J(w^n) \\ &\leq Var_{J \cup \{j-2\}}(w^n). \end{aligned}$$

which implies, since $\nu \in [0, 1]$

$$Var_J(w^{n+1}) = \nu |w_{j-2}^n - w_{j-1}^n| + |w_{j-1}^n - w_j^n| + (1 - \nu) |w_j^n - w_{j+1}^n| \quad (59)$$

$$\leq 2\nu \max\{|w_{j-2}^n|, |w_{j-1}^n|\} + Var_J(w^n)$$

To obtain a uniform bound for every time horizon let us take $T = N\Delta T$ and denote by \bar{M} the maximum number of switches at every iteration, clearly \bar{M} is bounded by the total number of nodes M in the (compact) support of the solution w^n (we can always assume that they are all contained in the interval $[a, b]$ and that $\Delta x = (b-a)/M$). Let us also denote by J_0^n the set of indices corresponding to the nodes where at time t_n there is no switch and by J_1^n the set of nodes where there is a switch. Clearly, at time t_n a node must belong either to J_0^n or to J_1^n . Let us consider number of elements is J_1 is \bar{M}_n . For every $0 < n \leq N-1$, we have

$$\begin{aligned} TV(w^{n+1}) &= \sum_{k \in J_0^n} |w_k^{n+1} - w_{k+1}^{n+1}| + \sum_{k \in J_1^n} |w_k^{n+1} - w_{k+1}^{n+1}| + \bar{M}_n \delta \Delta x \quad (60) \\ &\leq \sum_{k \in J_0^n \cup J_1^n} |w_k^n - w_{k+1}^n| + \bar{M}_n \delta \Delta x \\ &\leq \sum_{k \in J_0^n \cup J_1^n} |w_k^n - w_{k+1}^n| + M \delta \Delta x, \quad \text{since } \bar{M}_n \leq M \\ &\leq TV(w^n) + (b-a)\delta. \end{aligned}$$

Other possibility

$$\begin{aligned} TV(w^{n+1}) &= \sum_{k \in J_0^n} |w_k^{n+1} - w_{k+1}^{n+1}| + \sum_{k \in J_1^n} |w_k^{n+1} - w_{k+1}^{n+1}| \quad (61) \\ &\leq 2 \sum_{k \in J_0^n} |w_k^n - w_{k+1}^n| + \sum_{k \in J_1^n} |w_k^n - w_{k+1}^n| \\ &\leq TV(w^n) + \sum_{k \in J_0^n} |w_k^n - w_{k+1}^n| \\ &\leq TV(w^n) + \delta \Delta x \text{Card}(J_0^n) \\ &\leq TV(w^n) + \delta \Delta x M \\ &\leq TV(w^n) + (b-a)\delta. \end{aligned}$$

In both the cases we obtained the same bound.

$$\begin{aligned} TV(w^{n+1}) &= \sum_{k \in J_0^n} |w_k^{n+1} - w_{k+1}^{n+1}| + \sum_{k \in J_1^n} |w_k^{n+1} - w_{k+1}^{n+1}| \quad (62) \\ &\leq \sum_{k \in J_0^n} |w_k^{n+1} - w_{k+1}^{n+1}| + \sum_{k \in J_1^n} |w_k^n - w_{k+1}^n| + 2\bar{M}\nu \|w^n\|_\infty \\ &\leq \sum_{k \in J_0^n \cup J_1^n} |w_k^n - w_{k+1}^n| + 2\bar{M}\nu \|w^n\|_\infty = TV(w^n) + 2\bar{M}\nu \|w^n\|_\infty \end{aligned}$$

where we have used the fact that for $j \in J_0^n$ the total variation is non increasing. By the L^∞ bound proved in Proposition 1 we obtain $\|w^n\|_\infty \leq \|w^0\|_\infty$. Recalling the definition of ν , we iterate back to $n = 0$ obtaining

$$\begin{aligned} TV(w^{n+1}) &\leq TV(w^n) + 2\bar{M}\nu\|w^n\|_\infty \leq TV(w^0) + 2\bar{M}n\nu\|w^0\|_\infty \quad (63) \\ &\leq TV(w^0) + 2M^2c\frac{T}{b-a}\|w^0\|_\infty \end{aligned}$$

and this gives the uniform bound for the total variation. The proof for $\nu < 0$ can be easily adapted.

Case 4: $\sigma_j^n = 0$ and $\sigma_j^{n-1} = 1$. In addition, we assume that $\sigma_{j-1}^n = 0$. The scheme switches from the SL to UB scheme. We can first get a bound for the variation on the cell next to the x_j node by applying the projection P^{UB} . Then, we can divide the indices into two subsets as in Case 3, and we can obtain a similar upper bound on $TV(w^{n+1})$ by using the L^∞ bound for the UB scheme. The proof follows in the same way as in Case 3. \square

Proposition 3. *Let $|\nu| \leq 1$, then the coupled scheme $SL+UB$ is consistent with equation (39).*

Proof. Consistency is a local property and it will be inherited by the same property of the two schemes used to construct the coupled scheme because, as we will see below, the two projection operators are defined as centred averages.

Case 1: $\sigma_j^n = \sigma_j^{n-1} = 1$ no switch is needed. We already know that SL scheme is consistent and that is locally first order accurate (see [13] for details), so the property is true.

Case 2: $\sigma_j^n = \sigma_j^{n-1} = 0$ and no switch is needed. UB scheme is also consistent according to (10) (see [4] for details).

Case 3 : $\sigma_j^n = 1$ and $\sigma_j^{n-1} = 0$ so we switch from the UB scheme to the SL scheme. The property follows from the way we have defined the projection P^{SL} on the grid and the consistency of the SL scheme. We need to project on x_j , using (at most) the values at the neighbouring \times -nodes computed at the previous iteration (the index n is dropped for simplicity)

$$u(x_j) = \frac{\bar{u}_{j-1} + \bar{u}_j}{2}$$

Then, by construction,

$$u(x_j) = \frac{1}{2\Delta x} \int_{x_{j-1}}^{x_j} u(x)dx + \frac{1}{2\Delta x} \int_{x_j}^{x_{j+1}} u(x)dx = \frac{1}{2\Delta x} \int_{x_{j-1}}^{x_{j+1}} u(x)dx$$

Since $u(x_j)2\Delta x$ is the approximate value corresponding to the mid-point rule applied to the integral in $[x_{j-1}, x_{j+1}]$, for a regular function we get the following estimate

$$|u(x_j) - \frac{1}{2\Delta x} \int_{x_{j-1}}^{x_{j+1}} u(x) dx| \leq C\Delta x^2 \quad (64)$$

which, by the consistency of the SL scheme, guarantees the local consistency for the coupled scheme.

Case 4 : $\sigma_j^n = 0$ and $\sigma_j^{n-1} = 1$ so we switch from the SL scheme to the UB scheme. Now we need (at most) the values at the neighbouring \times -nodes with respect to x_j and they can be obtained by projection. The projection P^{UB} defines (again the index n is dropped for simplicity)

$$\bar{u}_j = \frac{u_{j+1} + u_j}{2}$$

so recalling that $\bar{x}_j = x_j + \Delta x/2$, we have

$$\min(u_j, u_{j+1}) \leq \bar{u}_j \leq \max(u_j, u_{j+1}) \quad (65)$$

For the definition of the fluxes of the UB scheme we will also need \bar{u}_{j-1} or \bar{u}_{j+1} but also for these values we will have similar bounds. This implies that the coupled scheme is consistent according to the definition (10). \square

4 Numerical tests

In this §, we present some numerical tests in one-dimension. We use different initial conditions with varying smoothness and track their time evolution over Ω . The coupled scheme improves the accuracy by switching between schemes using σ_j^n . The extra cost of computing σ_j^n is minimal as we only project the cells that switch. We start solving the advection equation with constant and variable velocity. Then, we give an example for an evolutive HJ equation (2) where, starting from a smooth initial condition, we follow the onset of a singularity at an intermediate time. We compare the proposed coupled scheme with the two schemes used as building blocks. To this end, we will consider several initial conditions with various regularity properties and we follow their evolutions in time over an interval Ω . We will compute the errors in $L^1(\Omega)$, $L^2(\Omega)$ and, in some cases, in $L^\infty(\Omega_{reg})$ to show also the behavior in the regular region. In our examples $\Omega_{reg} := \Omega \setminus \Omega_{sing}$ and $\Omega_{sing} := \cup_s B(\bar{x}_s, \varepsilon)$ where \bar{x}_s denotes a point where the derivative or the solution itself has a jump.

Example 1. Advection equation with constant velocity.

We consider the advection equation (39) where $c \equiv 1$ is the velocity and $v_0(x)$ is the initial condition with bounded support, $\Omega := (-2, 2)$, $T = 2$ and the Courant number $\nu = c\Delta t/\Delta x$ which remains constant at 0.9 throughout all the simulations. In this example, we explore two different initial conditions, referred to as (66) and (67).

Test 1: Smooth initial condition v_0 .

$$v_0(x) = \begin{cases} (1 - |x|^2)^4, & \text{for } |x| \leq 1 \\ 0 & \text{otherwise} \end{cases} \quad (66)$$

note that the derivative is 0 at the junction points $x = \pm 1$. It is clear that the solution remains smooth in the evolution hence the SL scheme should have a better accuracy with respect to the UB scheme. Moreover, since the slope is not high, we expect the coupled scheme to select always the SL scheme. Fig. 3, shows the solution of (39) at time $t = 20\Delta t$ with time step $\Delta t = 0.045$ for the initial data (66). Fig. 4 shows the plots of the switching parameter σ for different time $t = 10\Delta t, 20\Delta t, 30\Delta t$, with $\Delta t = 0.045$. As we expect, switching parameter $\sigma \equiv 1$ for the coupled scheme. Table 1 and 2 show the error tables for the UB and for the coupled scheme respectively. The error tables of the coupled and of the SL coincide on this test since the switching indicator is able to recognise that the solution is smooth enough and there are no jumps.

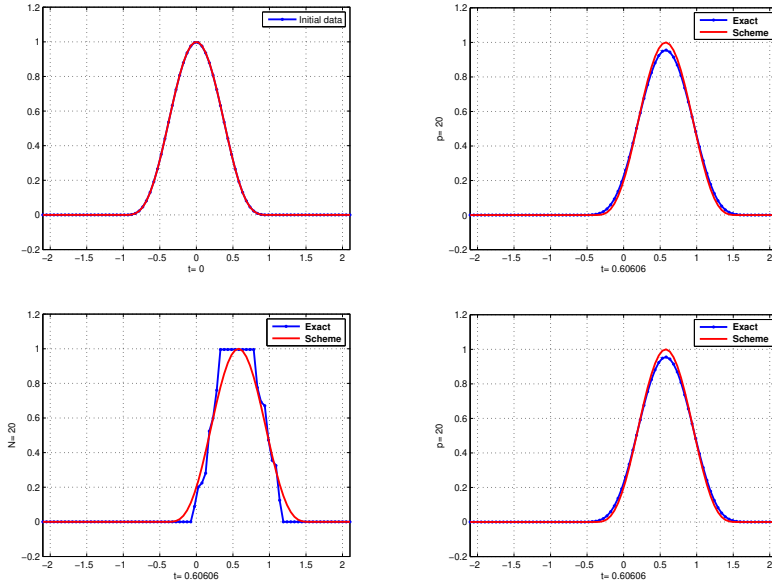


Fig. 3: Example 1, test 1: plots of the solutions for $t = 20\Delta t$, $\Delta t = 0.045$. Top: initial data (66) (left), SL scheme (right) and bottom: UB scheme (left), coupled scheme (right).

Test 2: Discontinuous initial condition v_0 .

$$v(0, x) = v_0(x) = \begin{cases} 1 & \text{if } |x| \leq 1 \\ 0 & \text{otherwise.} \end{cases} \quad (67)$$

For the piecewise discontinuous initial data UB scheme is already good so we expect the coupled scheme to switch to UB scheme. Fig. 5, shows the solution of (39) at time $t = 20\Delta t$ with $\Delta t = 0.045$ for the initial data (67). Fig. 6, shows the plots of σ for

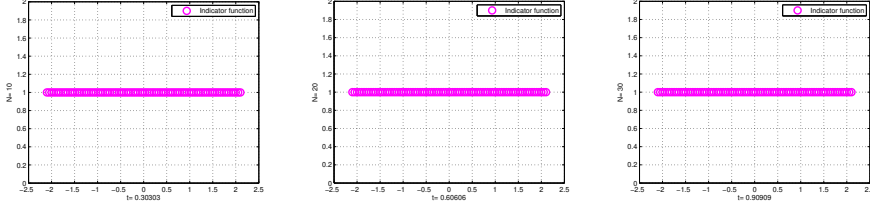


Fig. 4: Example 1, test 1: the plot of the indicator function σ at $t = 10\Delta t$, $20\Delta t$, $30\Delta t$ for $\Delta t = 0.045$.

Δt	Δx	L^1 Error	L^2 Error	L^∞ Error
0.181818	0.210526	9.04E-002	8.49E-002	1.10E-001
0.090909	0.102564	4.32E-002	4.27E-002	7.68E-002
0.045455	0.050633	2.17E-002	2.22E-002	5.56E-002
0.022472	0.025157	1.27E-002	1.27E-002	3.59E-002
0.011236	0.012539	6.49E-003	6.68E-003	2.20E-002
0.005634	0.006260	3.34E-003	3.50E-003	1.09E-002

Table 1: Example 1, test 1: errors for the UB scheme with initial condition (66) at time $T = 2$.

Δt	Δx	L^1 Error	L^2 Error	L^∞ Error
0.181818	0.210526	7.36E-002	5.93E-002	7.44E-002
0.090909	0.102564	3.49E-002	2.84E-002	3.64E-002
0.045455	0.050633	1.67E-002	1.37E-002	1.75E-002
0.022472	0.025157	8.87E-003	7.28E-003	9.31E-003
0.011236	0.012539	4.38E-003	3.60E-003	4.60E-003
0.005634	0.006260	2.14E-003	1.76E-003	2.25E-003

Table 2: Example 1, test 1: errors for the coupled $SL + UB$ scheme with initial condition (66) at time $T = 2$.

different times $t = 10\Delta t$, $20\Delta t$, $30\Delta t$ where $\Delta t = 0.45$. In Fig. 6, we can see that $\sigma = 0$ everywhere and hence coupled scheme is the same as UB scheme. Moreover one can see that once the scheme switches to the UB scheme ($\sigma = 0$) it keeps that choice on a larger number of cells in order to follow the jump. Tables 3 and 4, show the error tables respectively for the coupled, SL scheme respectively. Here coupled scheme is same as UB scheme.

Example 2. Advection with constant velocity and mixed initial conditions.

We consider the advection equation (39) with $c \equiv 0.1$ and $v_0(x)$ is an initial condition with compact support. In particular, we take an initial condition v_0 which contains

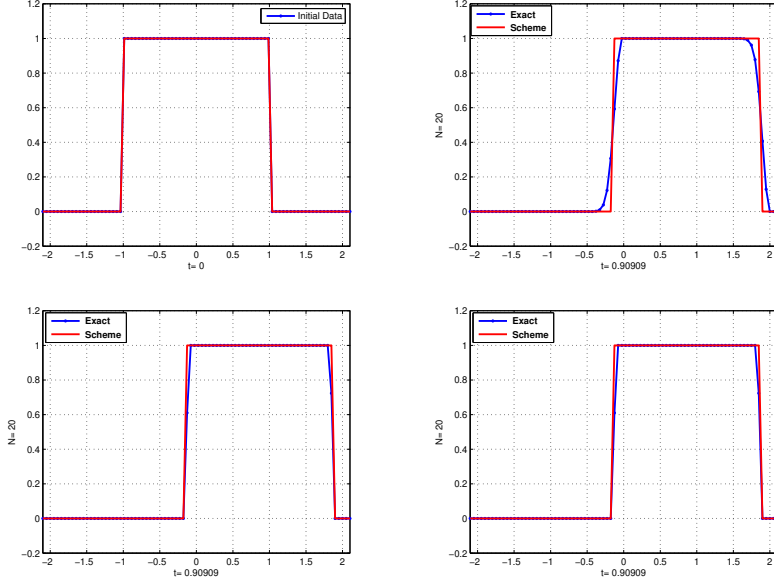


Fig. 5: Example 1, test 2: plots of the solutions for $t = 20\Delta t$, $\Delta t = 0.045$. Top: initial data (67) (left), SL scheme (right). Bottom: UB scheme (left), coupled scheme (right).

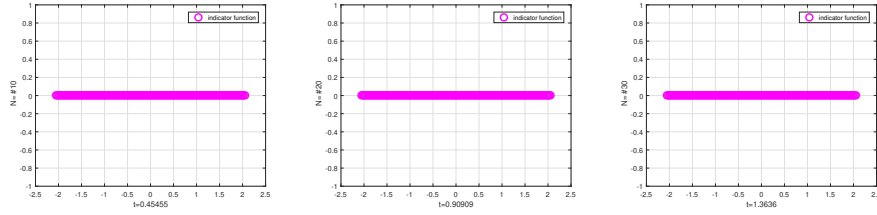


Fig. 6: Example 1, test 2: the plot of the indicator function σ for (67) at $t = 10\Delta t$, $20\Delta t$, $30\Delta t$ where $\Delta t = 0.045$.

Δt	Δx	L^1 Error	L^2 Error	L^∞ Error
0.181818	0.210526	7.02E-002	1.12E-001	2.12E-001
0.090909	0.102564	6.84E-002	1.51E-001	3.56E-001
0.045455	0.050633	3.38E-002	1.08E-001	3.90E-001
0.022472	0.025157	1.68E-002	8.32E-002	4.96E-001
0.011236	0.012539	8.36E-003	6.24E-002	5.44E-001
0.005634	0.006260	4.17E-003	3.73E-002	3.33E-001

Table 3: Example 1, test 2: errors for the $SL+UB$ scheme with initial condition (67) and $T = 2$.

three bumps

$$v(0, x) = v_0(x) = \begin{cases} 1 - |x + 3| & -4 < x < -2 \\ (1 - x^2)^4 & -1 < x < 1 \\ 1 & 2 < x < 3 \\ 0 & \text{otherwise,} \end{cases} \quad (68)$$

Δt	Δx	L^1 Error	L^2 Error	L^∞ Error
0.181818	0.210526	2.53E-001	3.32E-001	5.56E-001
0.090909	0.102564	1.43E-001	1.99E-001	3.38E-001
0.045455	0.050633	1.03E-001	1.72E-001	4.07E-001
0.022472	0.025157	7.57E-002	1.47E-001	4.05E-001
0.011236	0.012539	5.37E-002	1.25E-001	4.38E-001
0.005634	0.006260	3.77E-002	1.05E-001	4.61E-001

Table 4: Example 1, test 2: errors for the SL scheme with initial condition (67) at time $T = 2$.

In this test $\Omega = (-4.5, 4.5)$, $T = 6$ and $\nu = 0.0833$. Fig. 7 compares the different plots. Note that the SL scheme has a rather big error around the jumps, even where the solution is flat and has a larger support with respect to the exact solution. The UB has the typical piecewise constant behavior in the regularity region but keeps the support correctly. In Table 7 we show the errors for $L^1(\Omega)$, $L^2(\Omega)$, $L^\infty(\Omega)$ and $L^\infty(\Omega_{reg})$. It is clear that in this example initial data v_0 (68) have different regularity in different intervals so we expect to get small L^∞ errors only in the domain where the solution is regular, outside even a single node can make the L^∞ error increase. That is why that $L^1(\Omega)$ errors for the coupled scheme are close to those of the UB and the local $L^\infty(\Omega_{reg})$ error are better with respect to the SL scheme and UB scheme.

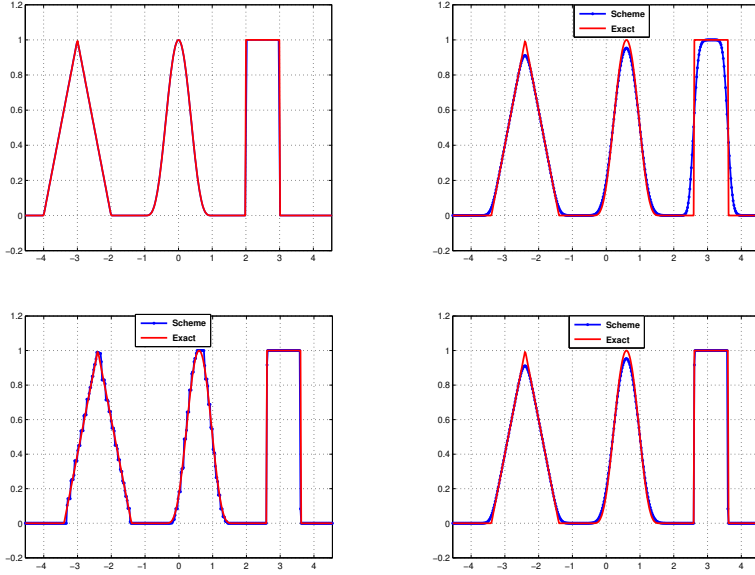


Fig. 7: Example 2, plot of the solutions at $T = 1$. Top: initial data (68) (left) and of SL scheme (right). Bottom: UB (left), coupled scheme (right).

Δt	Δx	L^1 Error	L^2 Error	L^∞ Error
0.0750	0.0900	4.16E-001	3.69E-001	9.16E-001
0.0375	0.0450	1.79E-001	1.27E-001	2.50E-001
0.0187	0.0225	9.82E-002	1.46E-001	9.16E-001
0.0094	0.0112	4.87E-002	8.87E-002	7.50E-001
0.0047	0.0056	2.34E-002	7.01E-002	9.16E-001

Table 5: Example 2, errors for *UB* scheme at time $T = 6$.

Δt	Δx	L^1 Error	L^2 Error	L^∞ Error
0.0750	0.0900	6.14E-001	3.61E-001	5.09E-001
0.0375	0.0450	3.99E-001	2.89E-001	5.44E-001
0.0187	0.0225	2.49E-001	2.34E-001	5.04E-001
0.0094	0.0112	1.62E-001	1.94E-001	5.22E-001
0.0047	0.0056	1.07E-001	1.62E-001	5.02E-001

Table 6: Example 2, errors for *SL* scheme at time $T = 6$.

Δt	Δx	L^1 Error	L^2 Error	L^∞ Error	$L^\infty(\Omega_{reg})$
0.0750	0.0900	3.49E-001	3.14E-001	9.16E-001	1.61E-001
0.0375	0.0450	1.60E-001	1.13E-001	2.50E-001	1.12E-001
0.0187	0.0225	9.41E-002	1.46E-001	9.16E-001	8.12E-002
0.0094	0.0112	4.79E-002	8.78E-002	7.50E-001	5.92E-002
0.0047	0.0056	2.41E-002	7.05E-002	9.16E-001	4.25E-002

Table 7: Example 2, errors for coupled *SL+ UB* scheme at $T = 6$.

Example 3. Advection equation with variable velocity.

In this example, we consider the advection equation with the variable velocity $c(x) = -(x - \bar{x})$, where $\bar{x} = 1.1$ (this example has been taken from [13]). We consider smooth initial data which has bounded second derivative i.e.

$$v(0, x) = v_0(x) = \max(0, 1 - 16(x - 0.25)^2)^2 \quad (69)$$

Here the domain $\Omega = (0, 1)$, $T = 1$ and we fix $\nu = 0.6$. As the solution is smooth, we expect our coupled scheme to coincide with *SL* everywhere. Fig. 8 shows the solution corresponding to (69) at time $t = 20\Delta t$ with the time step $\Delta t = 0.015385$ for the different schemes. As one can see the *UB* scheme has its typical stepwise approximation. Fig. 9 shows the plot of σ for different times $t = 10\Delta t, 20\Delta t, 30\Delta t$. The switching indicator is able to detect that the solution is smooth and chooses to apply the *SL* scheme in the whole domain. Comparing Tables 8 and Table 9 it can be seen that in this example the L^∞ error is much better for the *SL* (and coupled) scheme in particular for larger space/time steps and that the L^1 error is of the same order for *UB* and the coupled scheme.

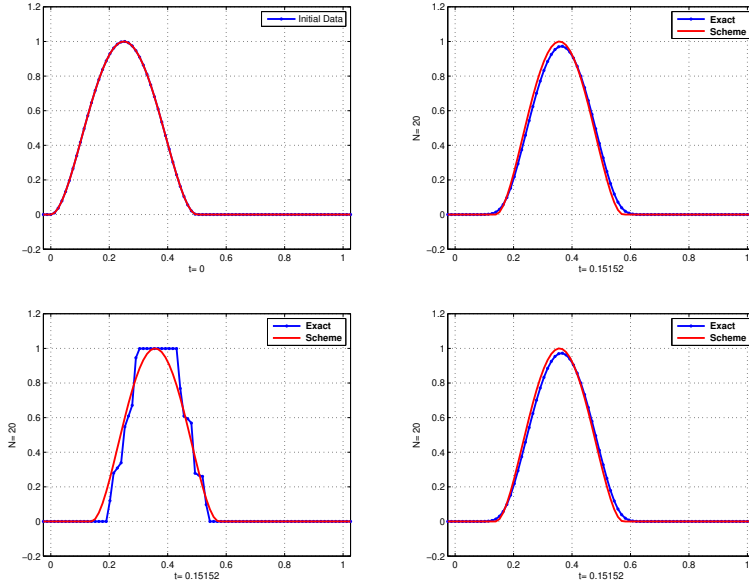


Fig. 8: Example 3: plot of the solutions at $t = 20\Delta t$ where $\Delta t = 0.015385$. Top: initial condition (left) and SL (right). Bottom: UB (left) and coupled scheme (right)

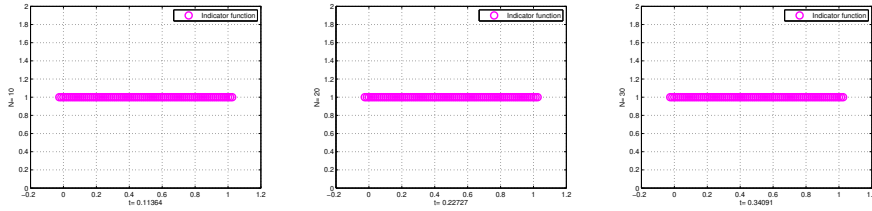


Fig. 9: Example 3, the plot of the indicator function σ for (69) initial data for $\Delta t = 0.015385$ and $t = 5\Delta t, 10\Delta t, 20\Delta t$.

Δt	Δx	L^1 Error	L^2 Error	L^∞ Error
0.031250	0.052632	5.07E-002	1.04E-001	3.04E-001
0.015385	0.025641	5.98E-002	1.15E-001	3.44E-001
0.007576	0.012658	3.08E-002	5.85E-002	2.12E-001
0.003774	0.006289	1.95E-002	3.72E-002	1.33E-001
0.001880	0.003135	1.58E-002	3.01E-002	1.18E-001
0.000939	0.001565	1.54E-002	2.74E-002	9.67E-002

Table 8: Example 3, errors for the UB scheme with initial condition (69) at time $T = 1$.

Δt	Δx	L^1 Error	L^2 Error	L^∞ Error
0.031250	0.052632	2.98E-002	4.50E-002	9.51E-002
0.015385	0.025641	1.95E-002	3.09E-002	6.63E-002
0.007576	0.012658	1.53E-002	2.52E-002	5.86E-002
0.003774	0.006289	1.52E-002	2.56E-002	6.16E-002
0.001880	0.003135	1.50E-002	2.53E-002	6.16E-002
0.000939	0.001565	1.51E-002	2.57E-002	6.29E-002

Table 9: Example 3, errors for the coupled $SL+UB$ scheme with initial condition (69) at time $T = 1$.

Example 4. Finally, let us consider the evolutive Hamilton-Jacobi equation

$$v_t + |cv_x| = 0 \quad (t, x) \in \Omega. \quad (70)$$

We take $c = 1$ and the smooth initial condition (66). Here the domain $\Omega = [-2, 2]$, $T = 0.5$ and we fix $\nu = 0.6$. In the tables, all the errors are global in Ω . In this case, the initial solution is smooth but at some point, the solution loses its regularity and a kink appears at $x = 0$. So at the beginning we expect the coupled scheme to apply the SL scheme and when at time t_n the singularity is detected the switching parameter σ_j^n becomes 0 in a cell and the coupled scheme must switch to the UB scheme. Fig. 10–12, show the plots at different time steps of the evolution of the same initial condition (66). Fig. 13, shows the evolution of the switching indicator which has the desired behavior, i.e. until $t = 10\Delta t$ solution is smooth (and $\sigma \equiv 1$ everywhere). After that time when the regularity is lost a singularity is detected and $\sigma = 0$ at $x = 0$, so the scheme switches correctly to the UB scheme. Table 11–10, show the error tables of SL , UB and coupled scheme respectively at time $t = 20\Delta t$ for $\Delta t = 0.014706$. It should be noted that in this example the coupled scheme is always more accurate with respect to the UB scheme and in general its accuracy is very close to the SL scheme, for small space/time steps it is almost identical to the SL scheme. This is probably due to the fact that the singularity stays at $x = 0$ and that the solution is still Lipschitz continuous.

Δt	Δx	L^1 Error	L^2 Error	L^∞ Error
0.125000	0.210526	2.34E-001	2.42E-001	3.28E-001
0.055556	0.102564	8.26E-002	1.27E-001	2.69E-001
0.029412	0.050633	3.86E-002	5.20E-002	1.30E-001
0.014706	0.025157	1.76E-002	2.27E-002	6.69E-002
0.007463	0.012539	8.59E-003	1.04E-002	3.31E-002
0.003731	0.006260	6.80E-003	8.58E-003	2.41E-002

Table 10: Example 4: errors for the UB scheme with initial condition (66) at time $T = 0.5$.

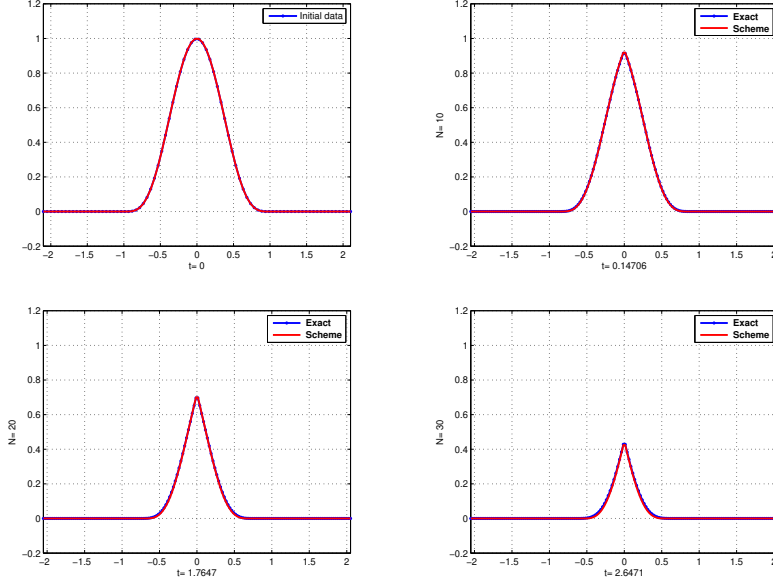


Fig. 10: Example 4, evolution of the initial condition (66) for the SL scheme at $t = 10\Delta t$, $20\Delta t$, $30\Delta t$, where $\Delta t = 0.014706$.

Δt	Δx	L^1 Error	L^2 Error	L^∞ Error
0.125000	0.210526	3.11E-002	2.62E-002	2.70E-002
0.055556	0.102564	2.27E-002	2.08E-002	2.52E-002
0.029412	0.050633	1.10E-002	1.01E-002	1.26E-002
0.014706	0.025157	5.96E-003	5.75E-003	7.45E-003
0.007463	0.012539	2.93E-003	2.85E-003	3.72E-003
0.003731	0.006260	1.47E-003	1.44E-003	1.89E-003

Table 11: Example 4: errors for the SL scheme with initial condition (66) at time $T = 0.5$.

Δt	Δx	L^1 Error	L^2 Error	L^∞ Error
0.125000	0.210526	5.01E-002	4.16E-002	4.27E-002
0.055556	0.102564	2.59E-002	2.35E-002	2.90E-002
0.029412	0.050633	1.16E-002	1.08E-002	1.36E-002
0.007463	0.012539	5.99E-003	5.71E-003	7.34E-003
0.014706	0.025157	2.98E-003	2.90E-003	3.79E-003
0.003731	0.006260	1.49E-003	1.46E-003	1.90E-003

Table 12: Example 4: errors for the coupled $SL+UB$ scheme with initial condition (66) at time $T = 0.5$.

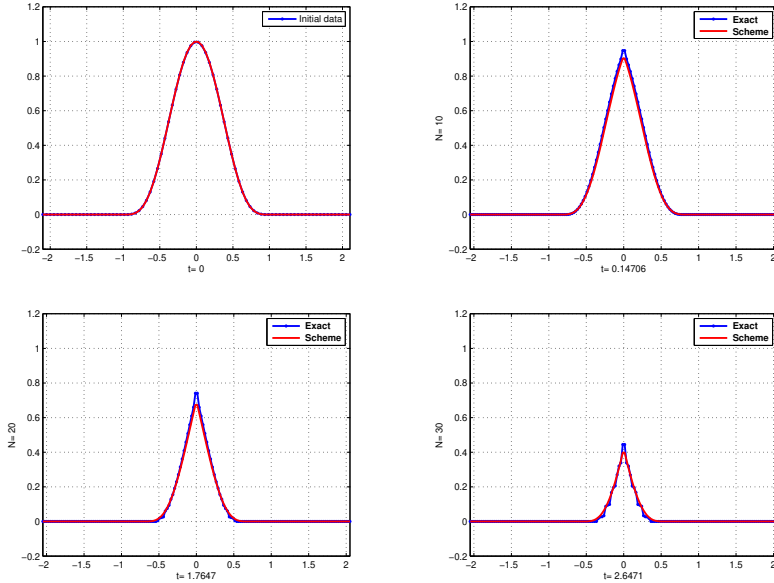


Fig. 11: Example 4: evolution of the initial condition (66) for the *UB* scheme at $t = 10\Delta t$, $20\Delta t$, $30\Delta t$, where $\Delta t = 0.014706$.

5 Conclusion and future work

In this paper, we recall the semi-Lagrangian [13], ultra-bee [7] schemes and coupled algorithm from [23] for solving advection and Hamilton-Jacobi equations. The scheme uses a switching indicator to decide which method to apply in each cell, depending on the smoothness and stability of the solution. We focus on the combination of an *SL* and *UB* method, and we show that the scheme can capture jumps and singularities accurately. The same idea of the scheme can be applied to other methods and can be simplified when the methods share the same grid and the same type of values, because then we do not need to project the values between different grids. We analyse the properties of the coupled scheme for the advection problem and we hope that they can be extended to non-linear Hamilton-Jacobi equations, as suggested by the last example. We plan to study this extension of the properties for HJ equation and the generalisation to 2D problems in future work.

Acknowledgements.

We dedicate this paper to my late PhD supervisor, Professor Maurizio Falcone, we started this work together few years ago. He was a great mentor. I am honoured to have worked with him and learned from him. His legacy will live on through his publications and many students.

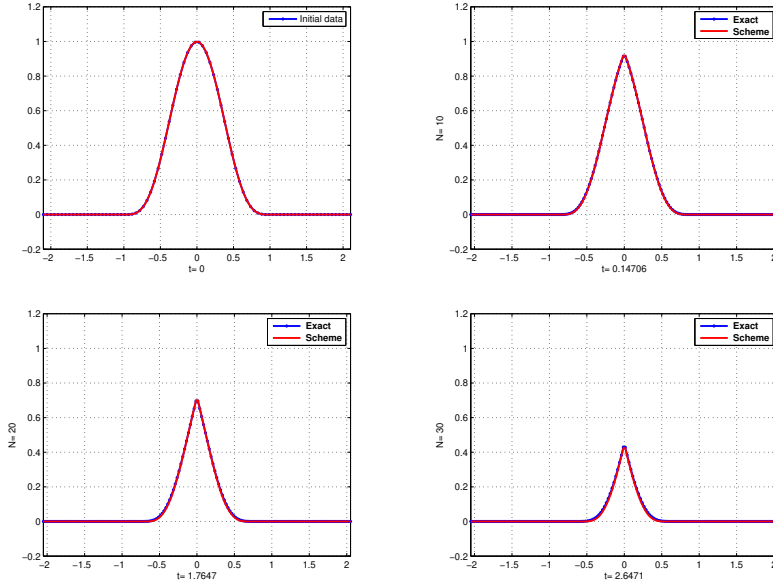


Fig. 12: Example 4, evolution of the initial condition (66) for the coupled $SL+UB$ scheme at $t = 10\Delta t, 20\Delta t, 30\Delta t$ where $\Delta t = 0.014706$.

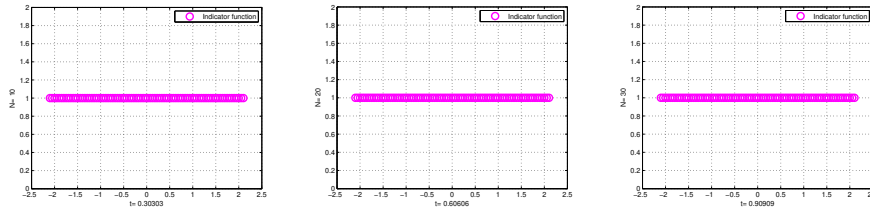


Fig. 13: Example 4, plot of the indicator function σ for (66) initial data at $t = 10\Delta t, 20\Delta t, 30\Delta t, \Delta t = 0.014706$.

Declarations

Ethical Approval

Not applicable.

Competing interests

The authors declare that they have no known competing financial interests or personal relationships that could have appeared to influence the work reported in this paper.

Author’s contributions

I am the only author, so I am responsible for this paper.

Funding

Not applicable.

Availability of data and materials

All data supporting the findings of this study are presented within this paper. There are no additional datasets associated with this research. Readers can find all relevant data, figures, and tables in the main body of the paper.

References

- [1] R. Abgrall. Construction of simple, stable and convergent hinge order scheme for steady first order Hamilton-Jacobi equation., *SIAM J. Sci. Comput.*, vol. 31, pp. 2419–2446, 2009.
- [2] M. Bardi and I. C. Dolcetta. *Optimal control and viscosity solutions of Hamilton-Jacobi-Bellman equations. Systems and Control. Foundations and Applications.* Birkhäuser, 1997.
- [3] G. Barles. *Solution de viscosité des équations de Hamilton-Jacobi.* Mathematiques et applications, 1994.
- [4] O. Bokanowski, N. Forcadel, and H. Zidani. l^1 -error estimates for numerical approximation of Hamilton-Jacobi-Bellman equation in dimension 1, *Math. Comp.*, vol. 79, pp. 1395–1426, 2010.
- [5] O. Bokanowski, M. Falcone, and S. Sahu. An efficient filtered scheme for some first order time-dependent Hamilton-Jacobi equations, *SIAM J. of Scient. Comput.*, vol. 38, no. 1, pp. 171–195, 2016.
- [6] O. Bokanowski, N. Megdich, and H. Zidani. Convergence of a non-monotone scheme for HJB equations with discontinuous initial data, *Numerische Math.*, vol. 115, no. 1, pp. 1–44, 2010.
- [7] O. Bokanowski and H. Zidani. Anti-dissipative schemes for advection and application to HJB equations, *J. Scient. Comput.*, vol. 30, no. 1, pp. 1–33, 2007.
- [8] S. Cacace, E. Cristiani, and R. Ferretti. Blended numerical schemes for the advection equation, *arXiv:1507.07092*, 2016.
- [9] R. Courant, E. Isaacson, and M. Rees. On the solution of nonlinear hyperbolic differential equations by finite differences, *Comm. Pure Appl. Math*, vol 5., pp 243–255., 1952.

- [10] M. G. Crandall and P. L. Lions. Two approximations of solutions of Hamilton-Jacobi equations., *Comput Methods Appl Mech Engrg*, vol 195., pp 1344–1386., 1984.
- [11] B. Despré and F. Lagoutière. Contact discontinuity capturing schemes for linear advection and compressible gas dynamics., *J Sci Comput*, vol 16., pp 479–524., 1999.
- [12] M. Falcone, G. Paolucci, S. Tozza. *Multidimensional smoothness indicators for first-order Hamilton-Jacobi equations*. Journal of Computational Physics, Volume 409, 2020.
- [13] M. Falcone and R. Ferretti. *Semi-Lagrangian Approximation Schemes for Linear and Hamilton-Jacobi Equations*. SIAM-Society for Industrial and Applied Mathematics, 2014.
- [14] M. Falcone and R. Ferretti. Discrete time high-order scheme for viscosity solutions of Hamilton-Jacobi equation, *Numer Math*, vol 67., p 315., 1994.
- [15] S. Gottlieb and C-W. Shu. Total variation diminishing Runge-Kutta schemes, *Math Comp*, vol 67., no 221., pp 73–85., 1998.
- [16] E. Godlewski and P. Raviart. *Numerical approximation of hyperbolic systems of conservation laws*. New York: Springer, 1996.
- [17] A. Harten. High resolution schemes for hyperbolic conservation laws, *J Comput phys*, vol 49., pp 357–393., 1983.
- [18] A. Harten., On a class of high resolution total-variation finite difference schemes, *SIAM J Numer Anal*, vol 21., pp 1–23., 1984.
- [19] G. Kossioris, C. Makridakis, and P. Souganidis. Finite volume schemes for hamilton-jacobi equations, *Numer Math*, vol 83., pp 427–442., 1999.
- [20] R. Leveque. *Numerical methods for conservation laws*. Basel: Birkhäuser, 1992.
- [21] C. B. Laney. *Computational Gasdynamics*. New York: Cambridge University press, 1998.
- [22] P. Roe. Some contributions to the modeling of discontinuous flows, *Lectures in App Math*, vol 22., pp 163–193., 1985.
- [23] S. Sahu. *Coupled Scheme for Hamilton–Jacobi Equations*. Klingenberg, C., Westdickenberg, M. (eds) Theory, Numerics and Applications of Hyperbolic Problems II. HYP 2016. Springer Proceedings in Mathematics & Statistics, vol 237. Springer, Cham.